THE UNIVERSITY OF ALABAMA IN HUNTSVILLE

FINAL REPORT

"Wavefront Analysis of Adaptive Telescope"

Submitted to:

NASA
Marshall Space Flight Center
Huntsville, Alabama

For:

Contract: NAS8-38609, D.O. 149

Submitted by:

James B. Hadaway
Center for Applied Optics
&
Lloyd Hillman
Dept. of Physics

March 1997

1. Introduction:

This report summarizes work performed by the University of Alabama in Huntsville (UAH) on the contract entitled "Wavefront Analysis of Adaptive Telescope" for NASA's Marshall Space Flight Center (contract NAS8-38609, Delivery Order 149).

The motivation for this work came from a NASA Headquarters interest in investigating design concepts for a large space telescope employing active optics technology. Current and foreseeable launch vehicles will be limited to carrying around 4-5 meter diameter objects. Thus, if a large, filled-aperture telescope (6-20 meters in diameter) is to be placed in space, it will be required to have a deployable primary mirror. Such a mirror may be an inflatable membrane or a segmented mirror consisting of many smaller pieces. In any case, it is expected that the deployed primary will not be of sufficient quality to achieve diffraction-limited performance for its aperture size. Thus, an active optics system will be needed to correct for initial as well as environmentally-produced primary figure errors.

Marshall Space Flight Center has developed considerable expertise in the area of active optics with the PAMELA test-bed. The combination of this experience along with the Marshall optical shop's work in mirror fabrication made MSFC the logical choice to lead NASA's effort to develop active optics technology for large, space-based, astronomical telescopes. Furthermore, UAH's support of MSFC in the areas of optical design, fabrication, and testing of space-based optical systems placed us in a key position to play a major role in the development of this future-generation telescope.

A careful study of the active optics components had to be carried out in order to determine control segment size, segment quality, and segment controllability required to achieve diffraction-limited resolution with a given primary mirror. With this in mind, UAH undertook the following effort to provide NASA/MSFC with optical design and analysis support for the large telescope study.

All of the work performed under this contract has already been reported, as a team member with MSFC, to NASA Headquarters in a series of presentations given between May and December of 1995. As specified on the delivery order, this report simply summarizes the material with the various UAH-written presentation packages attached as appendices.

2. Technical Approach:

The specific tasks to be associated with this effort were:

Task 1. UAH was to conduct a basic parametric study, based on the scientific mission and objectives to be specified by NASA, to determine the optical requirements of the telescope. This study was to consider the radiometry, field of view, resolution, wavelength range, pixel size, point-spread function, and exposure times that would affect the detection magnitude (size and intensity).

Task 2. UAH was to investigate the basic trade-offs of the optical configuration with active optical components. Possible designs to be considered were (a) two-mirror Cassegrain telescopes with an active primary and/or active secondary, and (b) four-mirror telescopes with an active tertiary and/or quaternary. The goal of this task was to achieve the telescope optical requirements determined above with the most practical and mechanically advantageous design possible.

Task 3. UAH was also to provide research to supplement MSFC's in-house efforts to develop concept options for a technology flight demonstration which could be used to prove the active/adaptive optics concepts for a large telescope.

Task 4. UAH was to present its findings of this study in meetings at MSFC and HQ as appropriate.

3. Telescope Optical Requirements Determination:

The first task was to select a baseline set of optical requirements for the telescope based on an analysis of the science requirements as well as trade-offs between performance and complexity/cost. It was clear from the earliest meetings on a large-aperture, actively-corrected space telescope,[1] that a combination of high light-gathering (i.e. large aperture), ultra-high resolution (milli-arc sec), large field-of-view (several arc minutes), and broad wavelength capability (UV-NIR) was desired by the scientific community. For most of these parameters, a factor of 2 to 10 improvement over the Hubble Space Telescope (HST) was desired.

Carl Pennypacker and John MacKenty of the Space Telescope Science Institute, put forth the optical requirements shown in Table 1 based on the science goals:[1]

Aperture diameter:	≥8 m
Waveband:	UV-VIS-NIR
FOV:	8 x 8 arc min
Resolution:	Diffraction-limited at 400 nm, or 0.010 arc sec.

Table 1. Basic optical requirements needed to meet baseline science goals.

Of particular interest was the telescope aperture diameter and configuration. Some of the desired scientific studies would require the collecting power of a 16-20 m diameter telescope. Thus, in order to investigate the worst-case situation and also provide 0.01 arc second resolution into the near-infrared, the baseline aperture diameter was set at 20 m. A roughly circular, filled aperture was selected as the baseline in order to give high light collection and a smooth modulation transfer function for the system. For such a large aperture, both a segmented primary that would be deployable and/or erectable and a deployable membrane primary were considered. For either primary, it was considered unrealistic that the optic could be deployed to and maintained within the positional tolerances required for high-resolution performance. Thus, it was planned that the primary

would be deployed as well as possible (to within many μm to mm) and an active mirror, located at a highly demagnified image of the primary, would be used to correct for deployment as well as environmentally-induced figure errors.

After discussions with the astronomers, it was realized that high-resolution imaging was required most in the near-infrared (NIR) waveband out to 3 microns. High throughput was more important in the ultraviolet (UV) and visible wavebands. This was one of the motivations for an aperture diameter of 20 m; this could provide 0.010 arc second resolution all the way out to 0.8 microns in the NIR. Thus, the system was designed to operate from the UV to 3 microns with the idea that the system tolerances would be set to insure diffraction-limited performance in the NIR.

The field-of-view was set at the desired 8 x 8 arc minutes for this study. In order to give two pixels (assuming 7 μm pixels) per plane-angle resolution element (four in two dimensions) as required using the Nyquist criterion, a telescope of 300 m effective focal length (F/15) is required. However, it should be noted that with these pixels, focal length, and FOV, a total of 10^{10} pixels would be required to fill the focal plane. Present projections put the maximum number of pixels on a single chip at around 10^8 over the next 5-7 years. Thus, while the desired optical performance may be achievable over such a wide field, the detector technology may not be available to actually utilize it.

As discussed above, the desired angular resolution was 0.010 arc seconds. Thus, this was set as the baseline geometrical resolution requirement for the study. This corresponds to diffraction-limited resolution at 0.8 microns for a 20 m aperture.

Table 2 summarizes the baseline optical requirements developed for the telescope.

Aperture diameter:	20 m
EFL, F/#:	300 m, F/15
Waveband:	UV to 3 μm
FOV:	8 x 8 arc min
Resolution:	≤ 0.010 arc sec, geometrically
Miscellaneous:	High throughput, good stray-light rejection, real image of primary within optical system.

Table 2. Baseline optical requirements for ULTIMA telescope.

Lastly, analysis showed that a space telescope with the above specifications could detect a star with a visual magnitude of 30 with an integration time of only 26 minutes (at a wavelength of 0.5 microns). This is quite reasonable.

4. Telescope Optical Design Concepts:

In the early stages, a basic two-mirror concept was investigated. The design started as a

Ritchey-Chretien (hyperbolic primary and secondary) to eliminate third-order spherical aberration and coma. Higher-order aspheric deformations were then applied to the primary and secondary in order to expand the usable FOV. However, astigmatism and field curvature are not fully correctable with the higher-order deformations and the desired resolution could only be achieved over a 1 arc minute full field. Based on this and the lack of a primary image, the two-mirror concept was not pursued.

Next, a four-mirror concept with a spherical primary developed by Korsch[2] was investigated. The original Korsch design was modified to conform to the requirements in Table 2. This design is shown in Appendix A. The four mirrors allow for excellent aberration correction over a large FOV even with the spherical primary and also provide for reimaging of the primary onto the quaternary. This early design showed promise with good resolution performance and excellent baffling characteristics. Also, the spherical primary would be easier to fabricate and could possibly be expanded on-orbit. However, the length of the system (38 m from the secondary to the image plane) was a problem. Thus, the F/2 primary needed to be made faster.

A second four-mirror design was developed with an F/1 primary. With the increased speed, it was not possible to keep the primary spherical. A parabolic primary was deemed realistic and was used. The total length of this system was only 26 m (20 m from primary to secondary). This concept is shown in Appendix B as the Type I design. The primary was again reimaged onto the quaternary. The required 0.01 arc second geometrical resolution was attained over most of an 8 arc minute full field using a curved image surface. The tertiary-quaternary-image plane section was designed to fit within the Shuttle cargo bay as a unit. With finite conjugates at both ends of this system, it could be built and tested as a unit on the ground, flown up in the Shuttle, and installed into the already-assembled and/or deployed primary-secondary structure. With most of the critical and more complex optical components in this smaller package, the risk could be reduced using this approach.

After the short, F/1 design was completed, there was concern as to whether a membrane primary could be made that fast. There was also a question as to whether a hole in the middle of a membrane was possible. Further discussions with JPL indicated that it was theoretically possible to fly two spacecraft to within mm and mrad positional accuracies. Thus, a separate design was developed specifically for a slower, continuous membrane primary. This concept is shown in Appendix B as the Type II design. The primary, still parabolic, was slowed to F/4.5. The secondary in the fast design was eliminated and the other two mirrors moved out in front of the primary to eliminate the hole. So, the primary would fly free of the secondary-tertiary-instruments package. The corrector mirror(s) would then be required to compensate for both primary errors and primary-secondary optics misalignments. With the slower primary, this would not be impossible. The separation between the primary and the secondary package is 90 m. The secondary-tertiary-image plane package is very similar to the tertiary-quaternary-image plane package in the Type 1 design. The optical performance of this design is slightly better than the Type I design (again, due to the slower primary). It achieves 0.01 arc second resolution over the full 8 arc minute field on a slightly curved image surface. The performance versus field for both designs with flat and curved image surfaces is shown in Appendix B.

To summarize, two optical designs were developed (one for a rigid, segmented primary and one for a membrane primary) that satisfy the baseline optical requirements. These designs were presented at the August review.[3] With additional study, one or both of these designs could be further optimized for use as a large-aperture space telescope.

5. Flight Demonstration Concepts:

Support was provided to the flight demonstration development effort in two ways. First, the various proposed concepts were checked for soundness from an optics perspective. This was done by reviewing presentation charts. Second, one demonstration concept was provided by UAH.

The objective for this precursor mission was understood to be a demonstration of active telescope technology on the Space Shuttle within a 2-3 year time frame and $5-20 million cost range. The key technologies that need to be demonstrated in space include light-weight, deployable mirrors, wavefront sensing, adaptive optics, and dynamic control systems. The proposed experiment would consist of a four-mirror, off-axis telescope with moderate resolution in the visible. The primary would be 0.5 to 1 m in diameter and consist of four deployable segments. A wavefront sensor would be located either behind a semi-transparent secondary or tertiary or at the final image plane. The quaternary would be located at an image of the primary and would have at least four segments for correction. The system would be pointed at a bright star (e.g. Sirius) as a perfect point source and first adjusted to give a good point-spread function on a high-speed, visible CCD. This would demonstrate the ability to correct for thermal and structural changes from ground to orbit. Then, the primary segments could be intentionally misaligned to see if the corrector could restore good image quality. Existing space-qualified hardware and software would be used as much as possible to reduce development time and cost. This concept was presented at the June review.[4]

6. Development of a Point Spread Function vs. Segmented/Active Mirror Analysis Tool:

6.1 Abstract

Segmented mirrors and/or discretely-actuated continuous mirrors will be a critical part of a large-aperture space telescope. Segmentation offer a method for achieving very large collection apertures, while "deformable" mirrors with a finite number of actuators provide the ability to actively compensate for on-orbit wavefront errors. For optimum performance, each element of such an array must be precisely aligned/controlled. Furthermore, the environment of space and the need to point and control the orientation of the telescope will subject the large support structure to stresses, torques and mechanical vibrations. The telescope will require an active control system to maintain the alignment of the mirrors. Errors in this alignment will degrade the image. There is a trade-off in the design between the size and number of elements in the array. This trade-off enters into many of the logistical decisions that affect the system's weight, assembly, transportation, heat dissipation, control complexity, cost, etc. Thus, a need was seen for an analysis tool that would allow for trades to be made between the number of segments/zones and individual segment/zone

control accuracy. This section describes the development of such a tool to show how the segment/zone alignment errors affect the optical performance of a telescope employing such an optic (as the primary and/or a corrector optic).

6.2 Background

For a well-corrected optical system, the point spread function (PSF) at a given wavelength is given by

$$PSF(x,y;\lambda) = \left| \int\int_{exit\ pupil} P(x',y') e^{-j(2\pi/\lambda)W(x',y')} e^{-j(2\pi/\lambda Z)(xx'+yy')} dx'dy' \right|^2 . \qquad (1)$$

In this equation P(x',y') is the aperture function of the exit pupil and W(x',y') is the wavefront aberration function (expressed in waves). Z is the distance from the exit pupil to the image plane. We note Eq. (1) is the squared modulus of the Fourier Transform of the complex exit pupil function

$$P(x',y') = P(x',y')\, e^{-j(2\pi/\lambda)W(x',y')} . \qquad (2)$$

For an astronomical telescope, this function characterizes how well the optical system transforms a plane wave (for an object at infinity) into a converging spherical wave. The aperture function P(x',y') tells how the telescope truncates the wave and the wavefront aberration function W(x',y') expresses the deviation of the wave from a true spherical wave.

Fourier analysis allows us to re-express Eq. (1) in another form. This form expresses the PSF as the Fourier transform of another function, namely the autocorrelation of the complex pupil function. The autocorrelation of the complex pupil function is given by

$$C(x',y') = P(x',y') \star P(x',y') = \int\int P^*(\alpha,\beta) P(\alpha+x',\beta+y') d\alpha d\beta \qquad (3)$$

which is Hermetian in x' & y' and symmetric about the origin. Its Fourier transform, which is the PSF, is therefore real,

$$PSF(x,y;\lambda) = \int\int C(x',y')\, e^{-j(2\pi/\lambda Z)(xx'+yy')} dx'dy' \qquad (4)$$

Equations (1) and (2) are general in that they apply even to the case of a segmented or active telescope. Segmentation or discrete actuation within the telescope pupil directly effects P(x',y'). Wherever there is a gap between segments, P(x',y') will be zero. The effect on the PSF of such regular gaps in say hexagonal or rectangular arrays of segments is well-understood and will not be discussed here, except to say that the gaps should be as small as possible. Furthermore, any imperfections in the figure of any segment will lead to variations of W(x',y') across the aperture. Again such aberrations are well-understood and must be addressed in the forming, figuring, and polishing of each segment. In this report, we will ignore the effects of gaps between segments and

will also assume that all segments have a perfect figure and shape. This leaves the final concern, namely the coherent alignment of all the segments or zones of a pupil optic. This is the topic of this section.

6.3 Errors & Issues

There are two primary concerns on the issue of alignment/phasing of a segmented/actuated optic. First, there is the issue of assembly. Perfectly aligning all the segments in the assembly stage presents a considerable challenge. This is compounded by the envisioned size of such a telescope and the environment in which they are to be assembled, namely space. Finally, once assembled, the large structure will be subjected to many and varying mechanical torques and thermal stresses. These forces undoubtedly will act to misalign the segments. Therefore, to align and maintain the coherent alignment of the segments, an active servo-control system is needed. This will consist of an electro-optic system that will measure and quantify the misalignment of each segment. This information is used to activate mechanical transducers that reposition the mirrors on the segmented primary and/or an actuated deformable corrector. This closed loop feedback system then actively maintains the alignment of all the segments or zones within the pupil.

As in any control system, there are many issues that affect its performance. Under the dynamically locked alignment, there will still be small positional errors for each segment or zone. These errors are directly a function of the gain, bandwidth, and complexity of the system. These in turn are directly related to the mechanical structure, the number of elements in the array, and the size of the individual elements. Overall, the errors will follow some complex, time-dependent statistical variation about the nominally perfect alignment states. In this analysis we investigate how such errors will affect the optical performance of the telescope.

The overall merit function for the design of a segmented telescope with active alignment and error correction has yet to be defined. Certainly the scientific objectives and hence the optical performance are a key element. If we assume that a minimum diameter is needed to meet the scientific objectives, then the merit function of the telescope design has a trade-off between the size and the number of segments/zones. The size versus number of segments/zones affects many things such as total mass, support structure, transportation, assembly, etc. If we just consider the servo-control system and the optical elements, we identify just a few advantages and disadvantages of both, as listed below.

Small Elements/Zones
Large single-element PSF.
More elements per fixed aperture size.
Complex control system.
Higher-order correction and control of aberrations.
Statistics of joint PSF with many segments.
Statistical limits and tolerance of alignment.
Tolerance of figure of single-element.

Large Elements/Zones
Small single-elements PSF.
Less elements per fixed aperture size.
Simpler control system.
Less correction and control of higher-order aberrations.
Statistics of joint PSF with few segments.
Statistical limits and tolerance of alignment.
Tolerance of figure of single-element.

6.4 Characterization of Alignment Errors

As stated previously, we only consider alignment errors. We assume that each segment or zone of the telescope is perfect in its figure. Furthermore, we assume that the design of the telescope is also perfect. Hence, when all the segments/zones are perfectly aligned, the telescope will transform a plane wave from a point source at infinity into a perfect truncated spherical wave in the telescope's exit pupil. In other words, we assume for the optical design that the wavefront aberration function is zero (i.e. $W(x',y') = 0$). Furthermore, since we are not allowing any gaps between adjacent elements, there are only two ways a single element can be misaligned. First, the element can be longitudinally shifted in its position out of its alignment plane. This leads to the aberration known as piston error. Across this displaced element, the piston error is constant. Because of the double-pass nature of reflective systems, the piston error induced by an element shifted ΔZ is $2\Delta Z$, or twice as much. The second type of misalignment is a tilting or planar rotation of an element. This leads to the aberration called tilt. Again, if the element is tilted by an amount $\Delta\theta$, the reflected wavefront across that element is tilted by $2\Delta\theta$. When expressed as a lateral change, the tilt across an element of width l is $l\Delta\theta$.

6.5 Modeling of Errors

The active alignment control system will attempt to drive the tilt and piston errors to zero. However, there is always some finite error. The size of this error depends on many factors such as the gain, bandwidth, and complexity. Realistically, we can only characterize these errors in a statistical fashion. Although there is bound to be some correlation and coupling between various elements, it is theoretically easier to treat the errors in each element as being statistically independent. We also assume that the error statistics are the same for each element. Given these assumptions, it is adequate to assume that the errors are normally distributed. This means that for a given servo gain, bandwidth, etc. the errors will be random with a Gaussian distribution. To characterize the error, we need only specify the rms deviation of the error, for the piston and for the tilt. This is the core assumption of the analysis.

6.6 Description of the Analysis Tool

Two programs were written using Mathcad® 6 Plus. The first is for a one-dimensional array. The second is for a two-dimensional square array. The one-dimensional program is used to calculate

the time-averaged point spread function. This corresponds to the effective PSF for a telescope when taking long exposures. In this case, long means that the integration time is much longer than the inverse of the width of the spectral density of the error fluctuations. This average is calculated from many ensembles using a Monte Carlo simulation. Piston and tilt with a random Gaussian distribution are assigned to each element. The PSF with these errors is then calculated. An average PSF is thus determined. An analytic solution to the one-dimensional array with Gaussian tilt and piston has also been found. The same procedure is used for the two-dimensional array, except that each ensemble is captured as a frame in an AVI computer video. This video gives a visual display of the twinkling of the star that may be observed.

6.7 Some Results Obtained Using the Analysis Tool

A full set of one-dimensional PSF results are shown in Appendix C. The first two plots show the difference between a twentieth-wave and a fifth-wave rms error distribution in piston and tilt for an aperture with 50 segments or zones. Each plot shows the PSF intensity in terms of visual magnitude units. Twentieth-wave (at any given wavelength of interest) gives a PSF that is very close to the ideal, while fifth-wave control shows significant PSF degradation. The next two plots show the difference between pure tilt error and pure piston error (with 50 zones and a fifth-wave of each aberration). Piston seems to be the worse of the two. For a segmented optic, the next plot shows the effect of a gap of 3/20 of the segment width between each of 50 segments with a fifth-wave of tilt and piston. When compared to the earlier plot of a fifth-wave of error with no gaps, one can see a significant degradation in the PSF. The next four plots show the effect of an increasing number of segments or zones (from 5 to 250) for a fixed total aperture width while holding the rms distribution of positional errors constant (at a tenth-wave). It is clear that the PSF will degrade with as the number of zones is increased. So, although more control over higher-order aberrations or figure errors is gained with a larger number of zones, the positional control accuracy required for each zone has to be improved as one adds zones in order to maintain the nominal performance of the system. This fact can not be overlooked when discussing the use of thousands or millions of segments and/or deformable mirror zones.

One frame from a two-dimensional video file is also shown in Appendix C indicating the effect of a fifth-wave rms piston error distributed over 8 x 8 zones of an optic (it should be noted that the intensity scale is log magnitude in the plots for easier visibility). In the actual video, the random fluctuations of the PSF are clearly seen.

6.8 Conclusion

An analytical modeling and analysis tool has been developed for simulating the performance of discretely-actuated adaptive optical components and systems. This tool can be used to evaluate segmented mirrors and/or discretely-actuated deformable mirrors with continuous face-sheets. The effects of segment/zone size, number, and control accuracy can be modeled and the quantitative results used to optimize a given system for a specific task. This analysis tool could be enhanced with the additional capability to model a wider range of surface errors such as micro-roughness and figure error within each zone. The mathematical framework of the model would allow for straightforward

inclusion of these errors.

7. Conclusion:

In support of NASA/MSFC's study of a large-aperture space telescope, UAH developed the telescope optical requirements based on the science goals, investigated potential optical design configurations for to meet the requirements, supplemented MSFC's efforts to develop concept options for a technology flight demonstration, and participated in meetings with MSFC to present the study results to NASA Headquarters.

Further work will be required in refining the optical requirements, optimizing the optical design, and selecting the optimum primary/corrector configuration. On the latter issue, a concept for a Power Spectral Density (PSD) function approach to matching a corrector to a primary was suggested (see end of Appendix C). Such an approach would provide a sound, quantitative rationale for selection of these components. Lastly, a continued study effort on future-generation space telescopes is required in order to drive out the critical technology issues that will be required to fly telescopes with apertures and resolutions that are well beyond what has been attainable in the past.

References:

1 E. E. Montgomery, compiler, *PAMELA Missions for Space Workshop*, MSFC, April 2-3, 1995.

2 D. Korsch, "Optical design considerations for next-generation space and lunar telescopes," SPIE Proc. 1494, p. 111 (1991).

3 E. E. Montgomery, compiler, *ULTIMA: Pre-Phase A Study Final Report*, MSFC, August 29, 1995.

4 E. E. Montgomery, compiler, *ULTIMA: Exploration of Concepts for a Space Proof-of-Principle of Active Segmented Optics*, MSFC, June 20-21, 1995.

Appendix A

UAH Input to
Interim ULTIMA Briefing
held on June 20-21, 1995
at MSFC (videocon)

Large Aperture Space Telescope Optical System Goals

- Large, expandable, filled aperture (up to 20 m) for high throughput and high resolution.
- Diffraction-limited theoretical performance at least in NIR (diff.-lim. resolution at $\lambda = 0.8$ μm & $D = 20$ m is 0.01 arc sec).
- Broad wavelength range (UV to IR).
- Large field of view (on the order of several arc min).
- Fast system (i.e. low F/#) to reduce length.
- Focal length optimized for low F/#, imager pixel size, and imager array size.
- Optical design favorable to baffling.
- Segmented components for transportability and expandability.
- Utilization of PAMELA active optics technology on at least one component (preferably two) to correct for assembly and environmentally-induced figure errors. Prefer PAMELA surface(s) to be on smaller diameter component(s).

4-Mirror Baseline Telescope

• Introduction

Two, three, and four mirror designs are possible for a large, filled-aperture telescope. Two mirror designs are limited to very small fields of view and put a heavy burden on the primary (in terms of shape & control). Three mirror designs do not perform as well as four and usually require four reflections anyway. Thus, a four mirror design by Korsch was studied as a baseline large-aperture telescope.

• Description

Primary:	Up to 20 m, F/2, spherical.
Secondary:	1/4 diam. of prim., conic.
Tertiary:	1/5 diam. of prim., asphere.
Quaternary:	1/20 diam. of prim., asphere.
Length:	Prim.-Sec. = 1.5 x prim. diam.
	Sec.-Img. = 1.9 x prim. diam.
FOV:	± 5 arc min.
F/#:	15.
Performance:	Near diff.-limited at 0.8 μm.

11:06:43

KORSCH 4-MIRROR ACONIC Scale: 0.0055 UAH 7-Jun-95

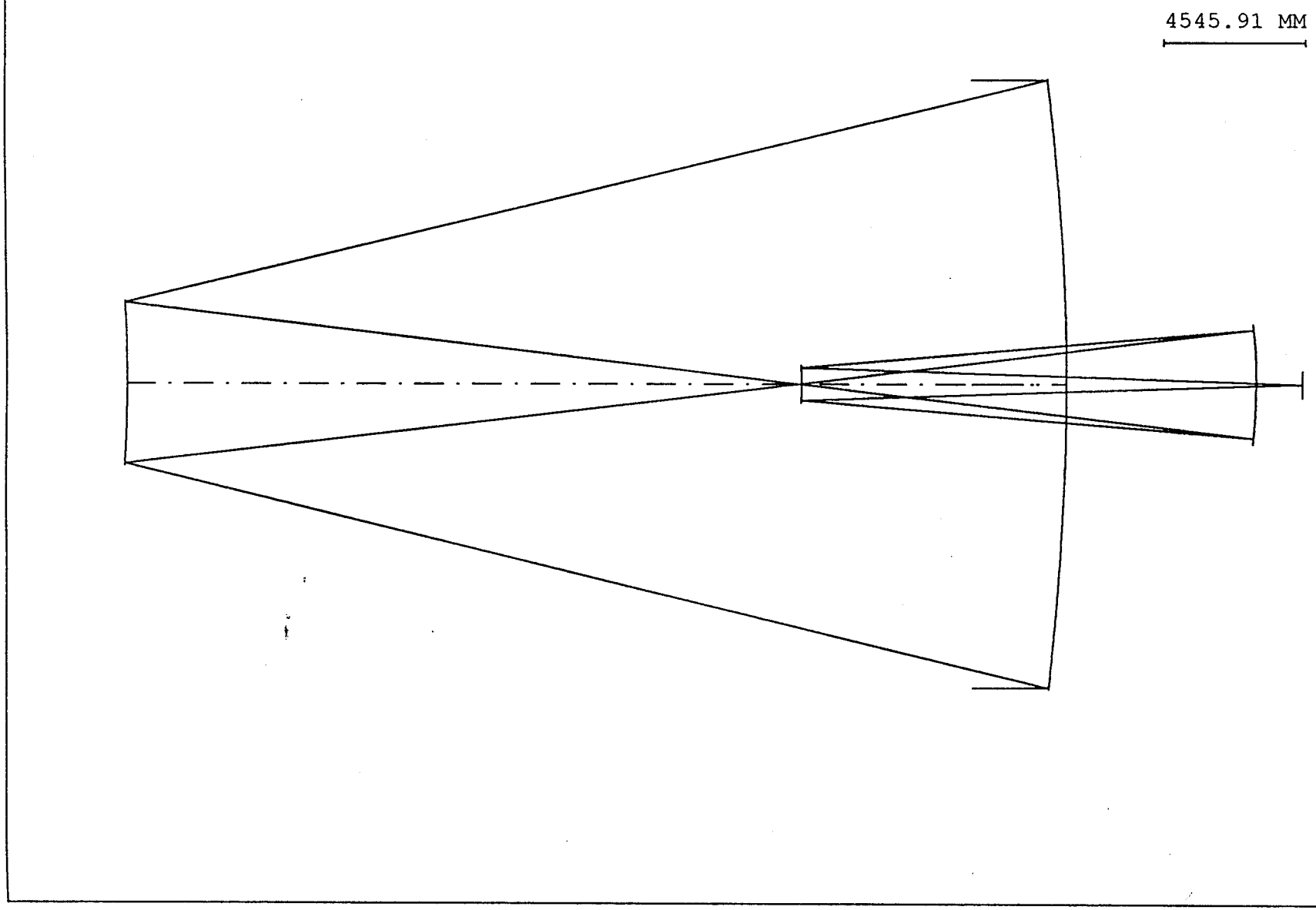

4-Mirror Baseline Telescope

- Advantages
  - Easily scalable/expandable with segmented, spherical primary.
  - Excellent performance.
  - Large field of view.
  - Excellent baffling capability.
  - PAMELA surface(s) can be placed on tertiary and/or quaternary. Tertiary/quaternary package fits into shuttle bay as a unit even with 20 m primary.
- Limitations
  - Overall length needs to be shortened (faster primary).
  - Four mirrors increases mechanical complexity and may limit throughput at some wavelengths.
- Summary

Korsch 4-mirror design is a good starting concept that demonstrates the feasibility of a large aperture active space telescope and highlights the key technological issues associated with such an undertaking.

Appendix B

UAH Input to
Final ULTIMA Briefing/Report
held on August 29, 1995
at MSFC

Optical System Goals

Requirements (based on science goals):

- Aperture diameter $\geq$ 8 m w/ 20 m desired.
- Resolution $\leq$ 0.01 arc sec (50 nrad).
- Field of View = 8 x 8 arc min.
- Spectral Range - UV to 3 μm.
- High throughput.
- Good baffling characteristics.

Resulting Optical System Specifications for Study Designs:

- Aperture diameter = 20 m (gives 0.01 arc sec resolution into IR).
- F/15 (gives >2 pixels/resol.-elem. w/ 7 μm pixels).
- More than 2 mirrors to correct field aberrations.
- Active optics in system to correct for primary surface errors, assembly errors, and dynamic disturbances. Requires imaging of primary on another mirror.
- Small primary obscuration.
- Internal field stop (image).

Type I - Fast Primary, Short Design

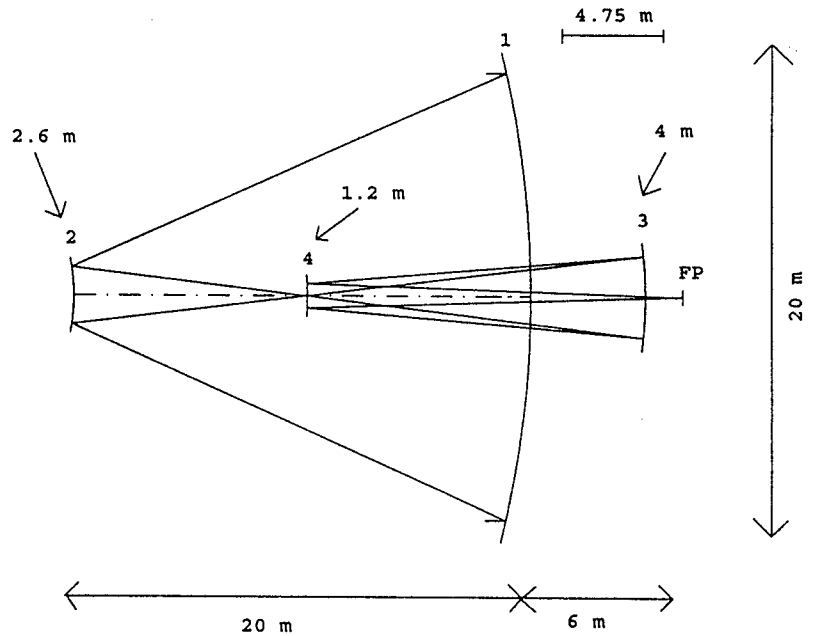

- Single structure/spacecraft.
- 4-mirror Korsch-type design.
- F/15 system.
- Parabolic primary (F/1), hyperbolic secondary, aconic tertiary, & aconic quaternary.
- 20 m long.
- 0.01 arc sec performance on curved image surface (rad = 5.3 m).
- Image of primary at quaternary & internal field stop.

Type II - Slow Primary, Long Design

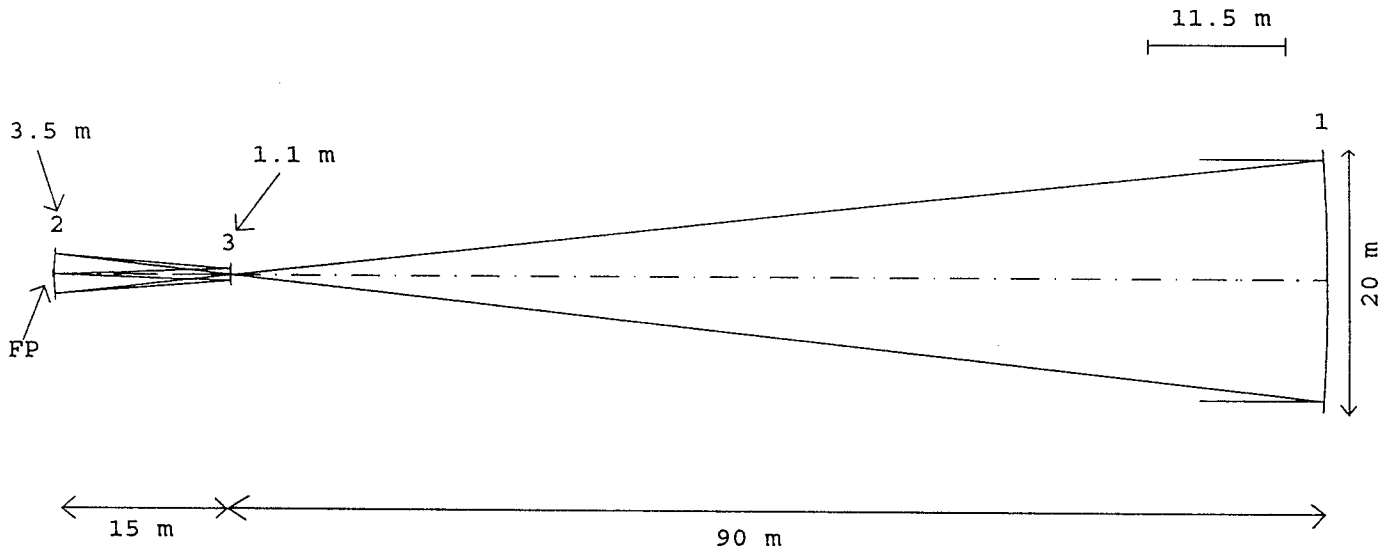

- Separate structures/spacecraft (alignment?).
- 3-mirror Korsch-type design w/ old secondary eliminated.
- F/15 system.
- Parabolic primary (F/4.5), aconic secondary, & aconic tertiary.
- 90 m between sections; 15 m from secondary to tertiary.
- 0.01 arc sec performance on curved image surface (rad = 28 m).
- Image of primary at tertiary & internal field stop.

Size Comparison

Type I

12.5 m

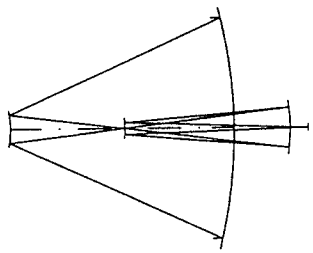

Type II

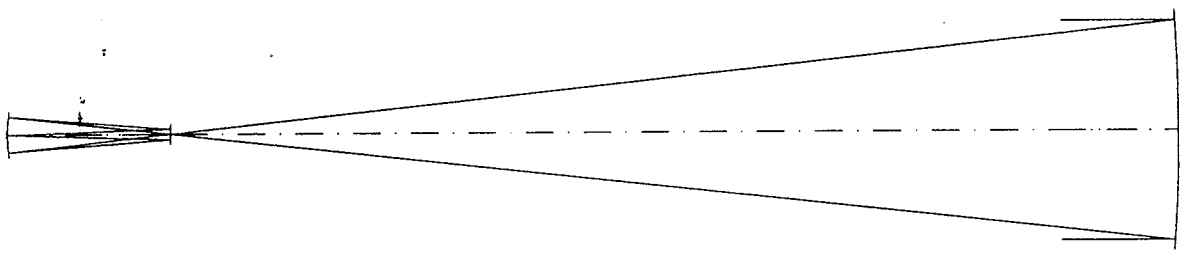

Performance vs. Field

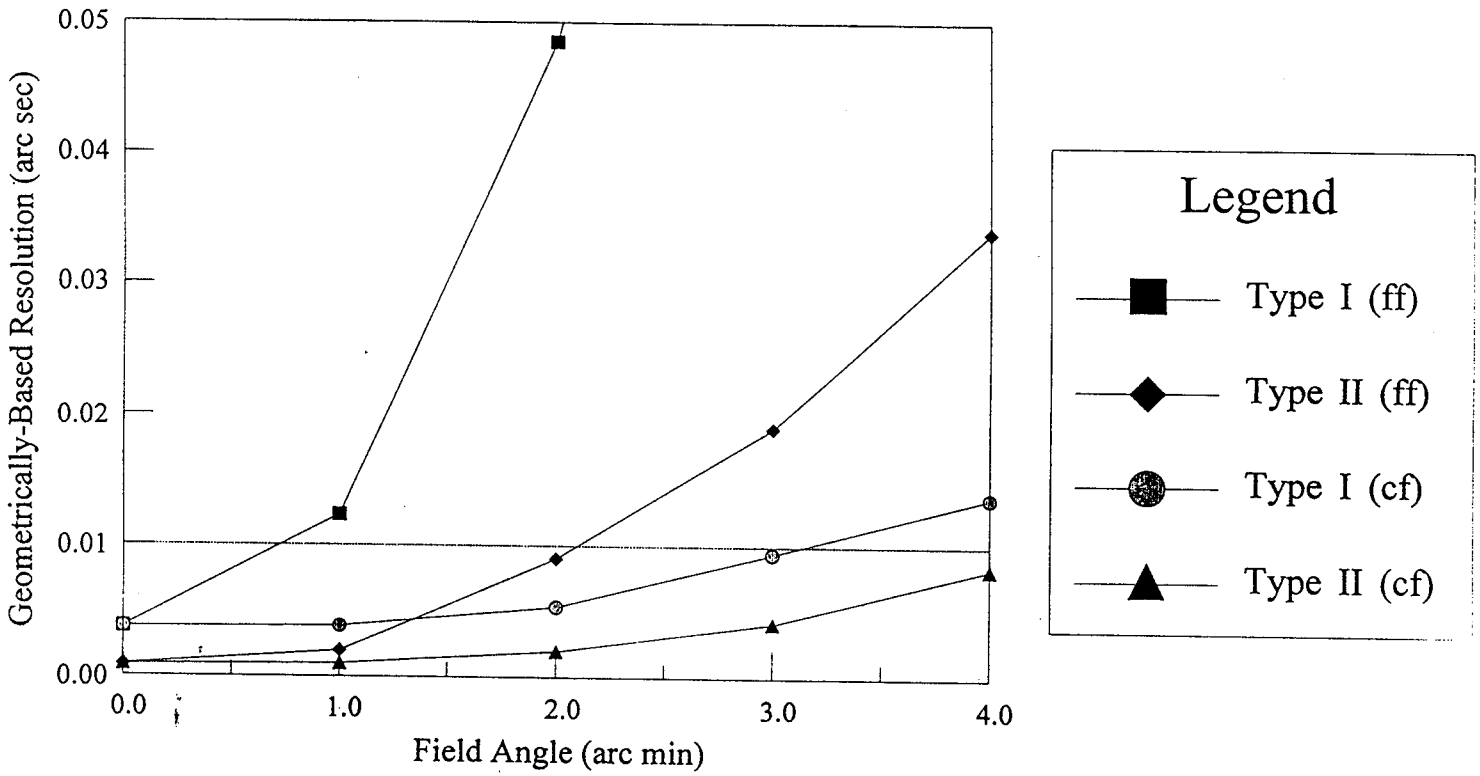

Appendix C

UAH Input to
Follow-up ULTIMA Briefing
held on December 13, 1995
at MSFC

Continuing UAH Analyses in Support of a Large Aperture Space Telescope

Topics to be Discussed:

I. Brief summary of Dr. Lloyd Hillman's work on modeling of discretely-actuated adaptive optical components.

II. Outline of a proposed Power Spectral Density (PSD) function approach to optimum corrector selection.

J.B. Hadaway, UAH, 12/13/95

Purpose of Dr. Hillman's Work

- Develop an analytical model for simulating the performance of discretely-actuated adaptive optical components/systems.

- Calculate Point Spread Function (PSF) given number of actuated zones over a normalized pupil, separation of non-continuous zones, and the distribution of piston & tilt errors across the zones. Efficiently done using Fourier transform:

$$PSF(x',y';\lambda) = \left| \int\int P(x,y) e^{-j(2\pi/\lambda)W(x,y)} e^{-j(2\pi/\lambda Z)(xx'+yy')} dxdy \right|^2$$

- Start with 1-dimensional model and then extend to 2 dimensions.

Gausian Distribution--Piston & Tilt

Plot Window Size :k $k := NN - 2500 .. NN + 2500$ Ensembles Averaged:M $M \equiv 100$

Number of Segments:E $E \equiv 50$

RMS Error: $Error \equiv \frac{2 \cdot \pi}{20}$

$2.5 \cdot \log(PSF_k + .00001)$

$2.5 \cdot \log(APSF1_k + .00001)$

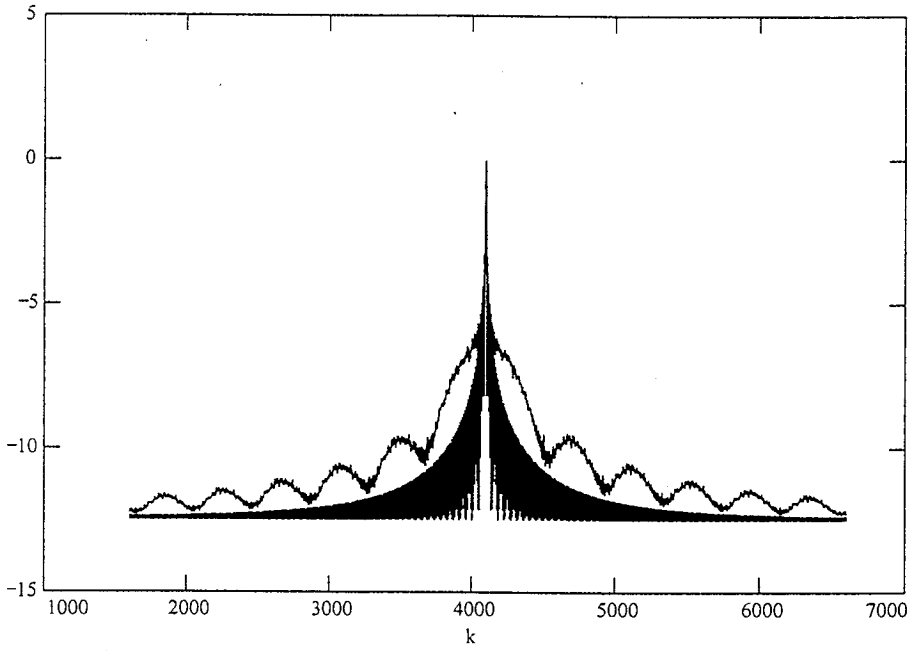

Ideal Aperture PSF Log Magnitude
Semented Aperture PSF Log Magnitude

$2.5 \cdot \log(\Delta PSF_k + .001)$

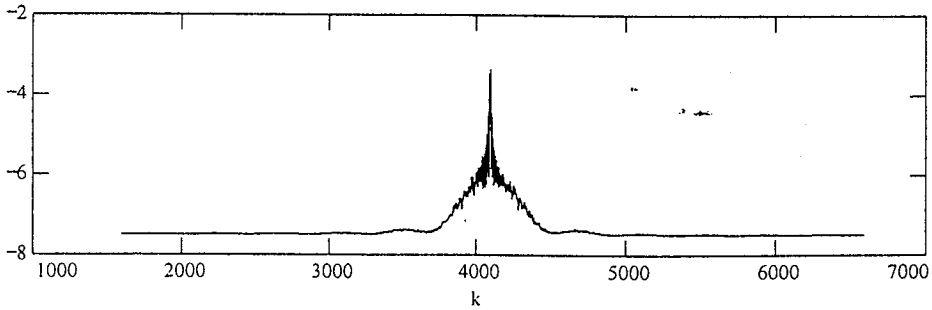

Gausian Distribution--Piston--& Tilt

Plot Window Size :k $k := NN - 2500 .. NN + 2500$ Ensembles Averaged:M $M \equiv 100$

Number of Segments:E $E \equiv 50$

RMS Error: $Error \equiv \frac{2 \cdot \pi}{5}$

$2.5 \cdot \log(PSF_k + .00001)$

$2.5 \cdot \log(APSF1_k + .00001)$

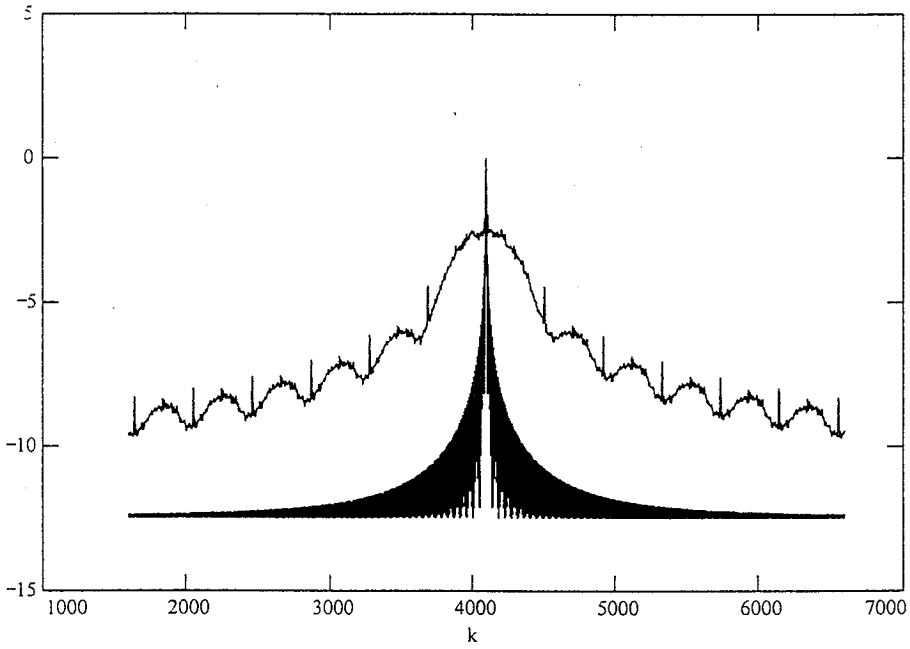

$2.5 \cdot \log(\Delta PSF_k + .001)$

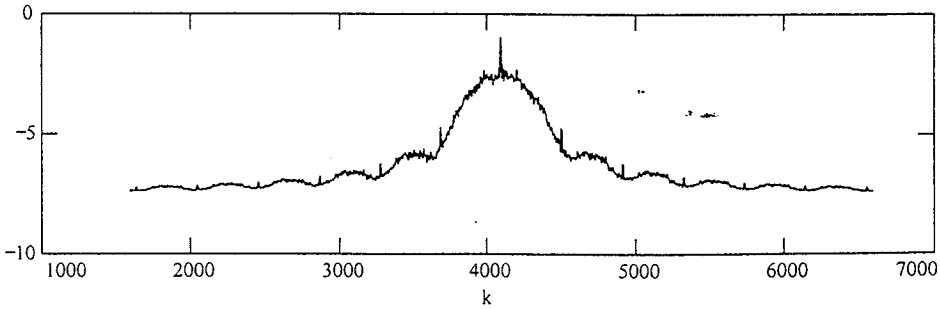

Gausian Distribution--No Piston-- Tilt

Plot Window Size :k $k := NN - 2500 .. NN + 2500$ Ensembles Averaged:M $M \equiv 100$

Number of Segments:E $E \equiv 50$

RMS Error: $Error \equiv \frac{2 \cdot \pi}{5}$

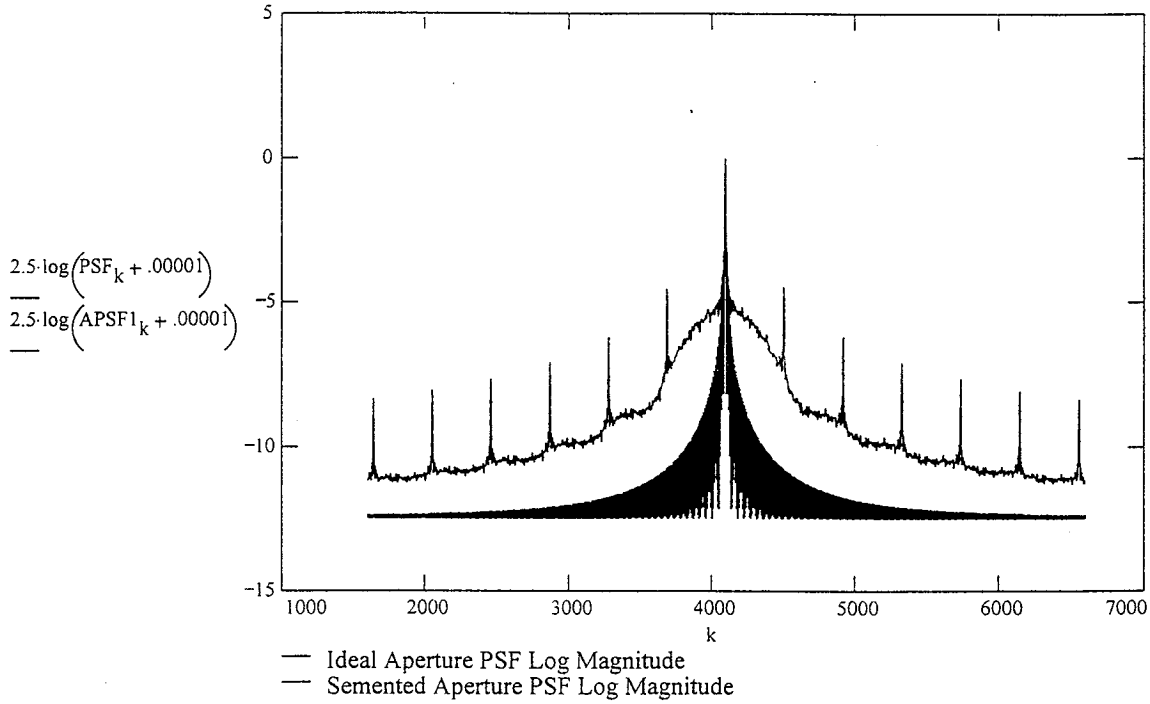

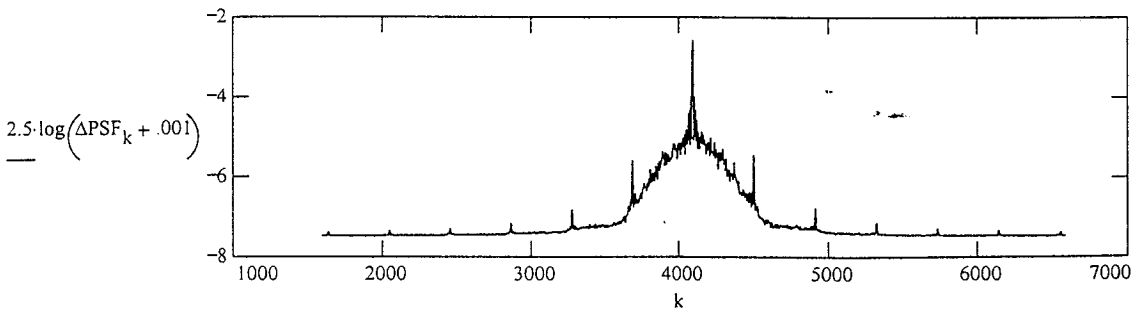

Gausian Distribution--Piston--No Tilt

Plot Window Size :k $k := NN - 2500 .. NN + 2500$ Ensembles Averaged:M $M \equiv 100$

Number of Segments:E $E \equiv 50$

RMS Error: $Error \equiv \frac{2 \cdot \pi}{5}$

$2.5 \cdot \log\left(PSF_k + .0001\right)$

$2.5 \cdot \log\left(APSF1_k + .0001\right)$

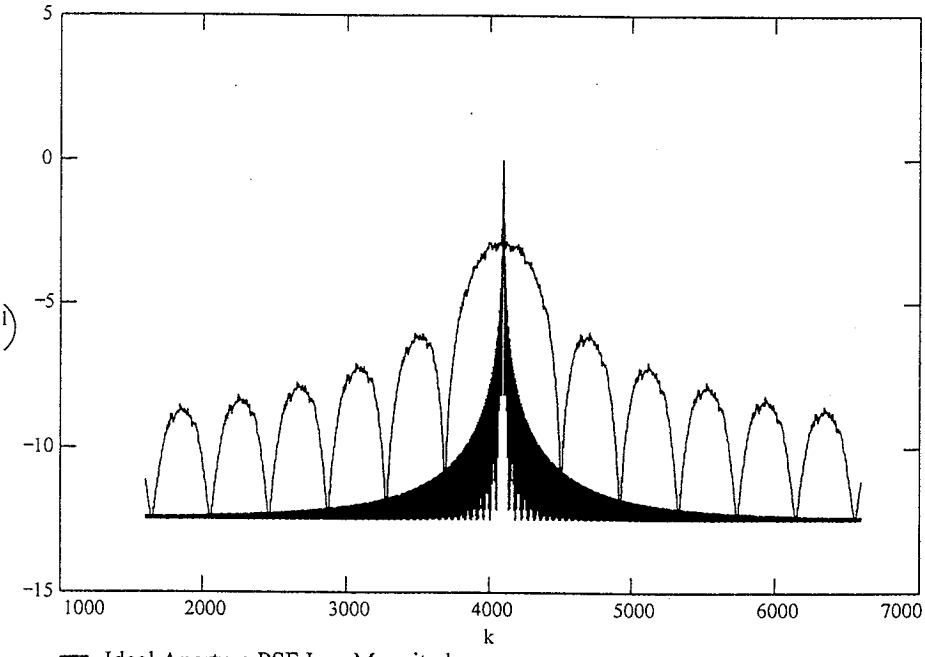

— Ideal Aperture PSF Log Magnitude
— Semented Aperture PSF Log Magnitude

$2.5 \cdot \log\left(\Delta PSF_k + .001\right)$

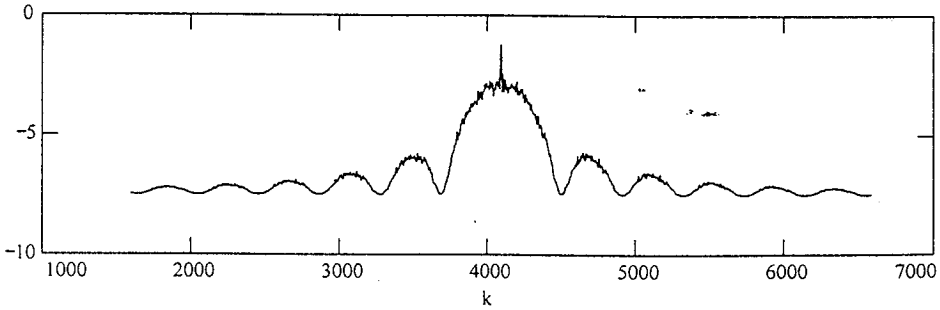

Effect of Segment Edges-- Tilt-- and Piston Width=3 out of 20

Plot Window Size :k $k := NN - 2500 .. NN + 2500$ Ensembles Averaged:M $M \equiv 100$

Number of Segments:E $E \equiv 50$

RMS Error: $Error \equiv \frac{2 \cdot \pi}{5}$

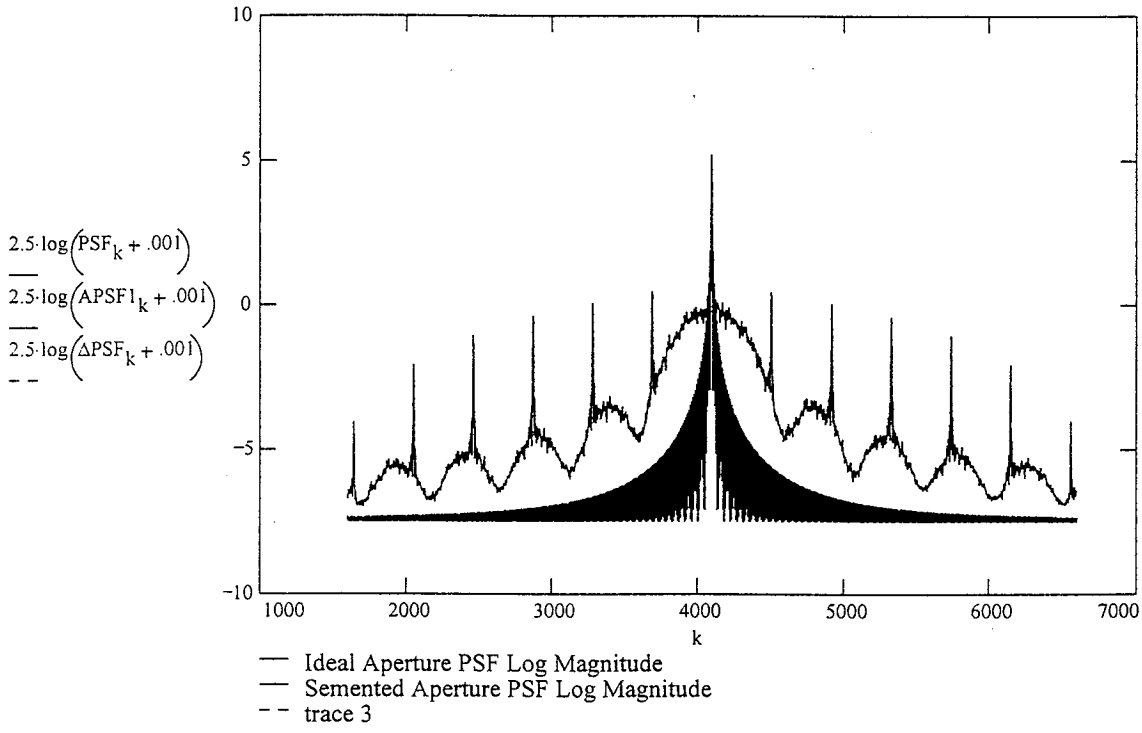

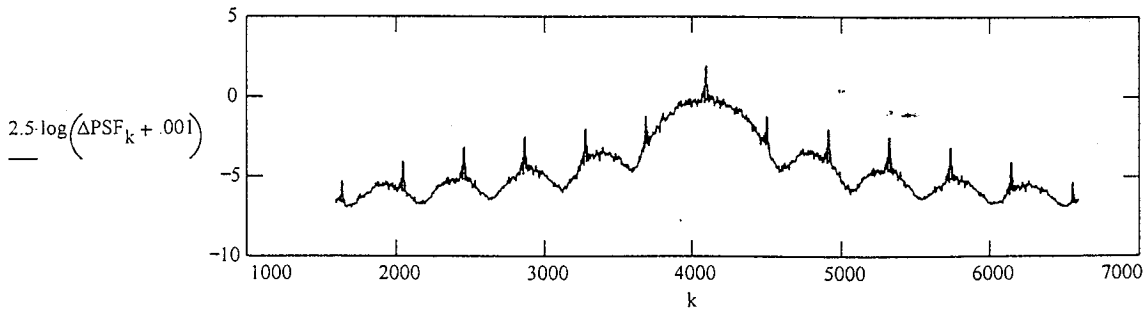

Plot Window Size :k $k = NN - 2000 .. NN - 2000$ Ensembles Averaged:M $M \equiv 50$

Number of Segments:E $E \equiv 5$

RMS Error: $Error \equiv \frac{2 \cdot \pi}{10}$

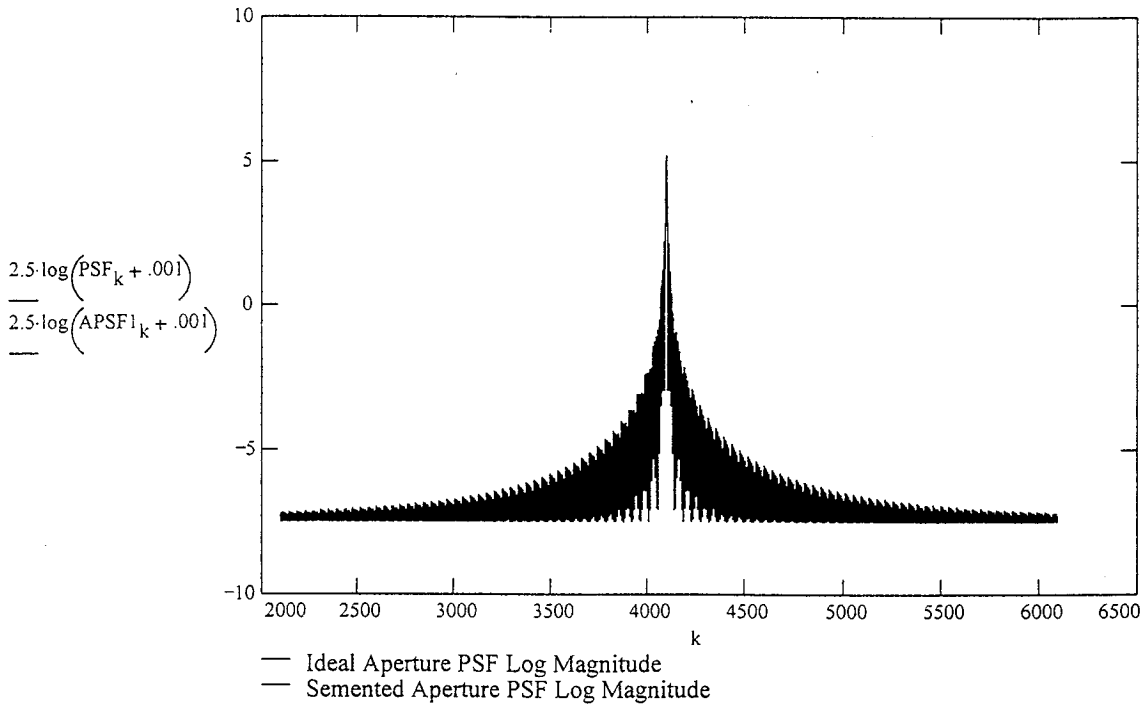

Plot Window Size :k $k := NN - 2000 .. NN + 2000$ Ensembles Averaged:M $M \equiv 50$

Number of Segments:E $E \equiv 25$

RMS Error: $Error \equiv \frac{2 \cdot \pi}{10}$

$2.5 \cdot \log\left(PSF_k + .001\right)$

$2.5 \cdot \log\left(APSF1_k + .001\right)$

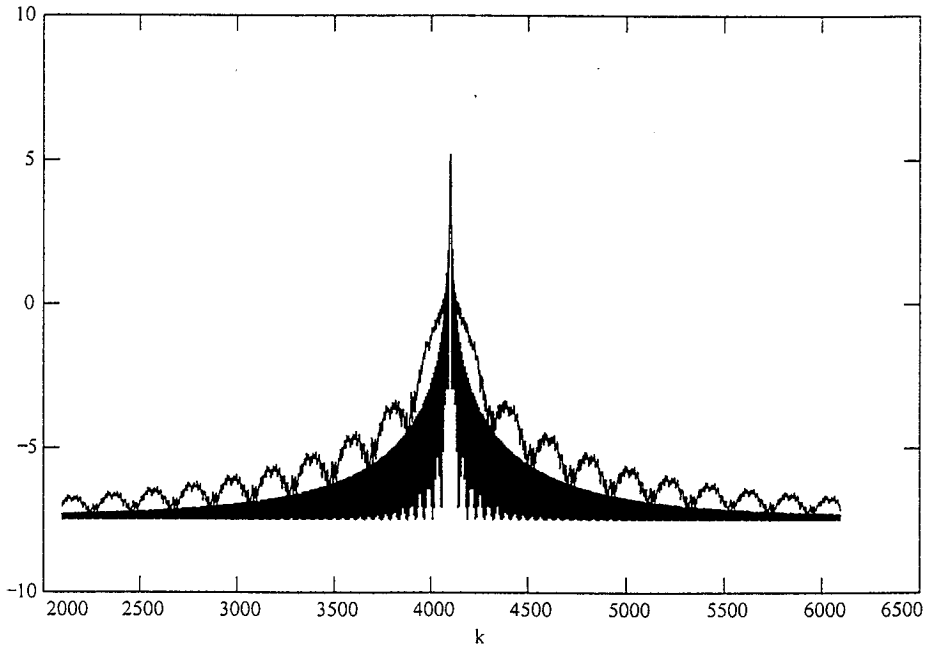

— Ideal Aperture PSF Log Magnitude

— Semented Aperture PSF Log Magnitude

Plot Window Size :k $k := NN - 2000 .. NN + 2000$ Ensembles Averaged:M $M \equiv 200$

Number of Segments:E $E \equiv 100$

RMS Error: $Error \equiv \frac{2 \cdot \pi}{10}$

$2.5 \cdot \log(PSF_k + .001)$

$2.5 \cdot \log(APSF1_k + .001)$

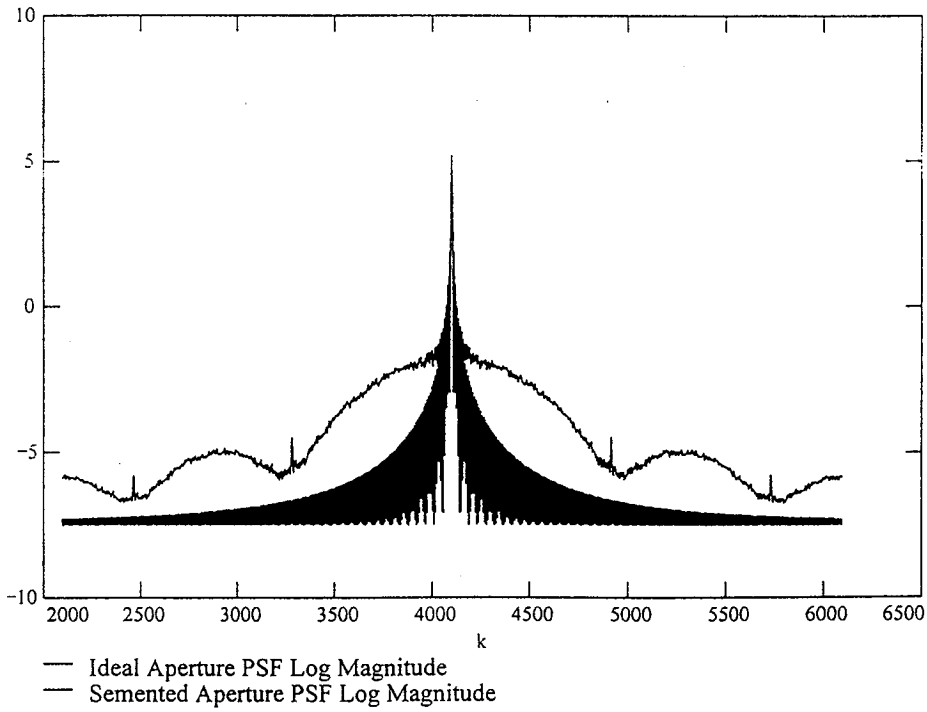

Plot Window Size :k $k := NN - 2000 .. NN + 2000$ Ensembles Averaged:M $M \equiv 50$

Number of Segments:E $E \equiv 250$

RMS Error: $Error \equiv \frac{2 \cdot \pi}{10}$

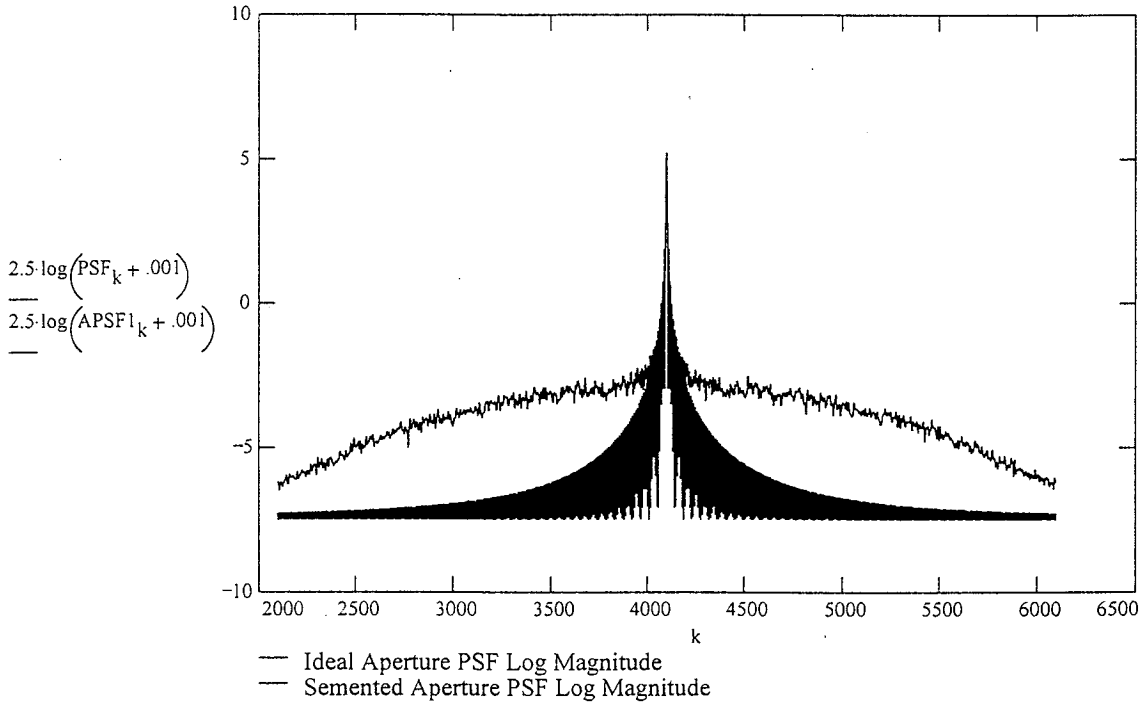

2-D Example: Square Aperture 8x8 Array
$\lambda/5$ RMS Piston Error Gaussian Ditributed

Log Magnitude Intensity

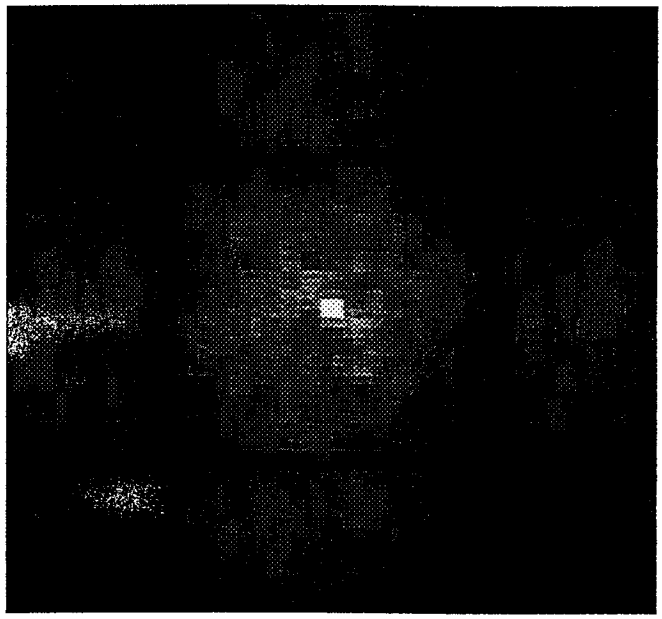

Piston=$\lambda/5$ rms

B1

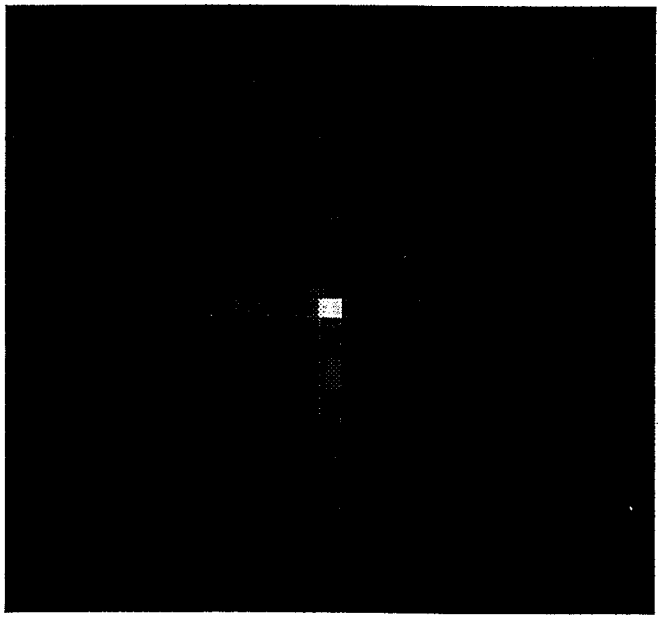

"Ideal" Image

B2

Graphical Summary of Various Effects

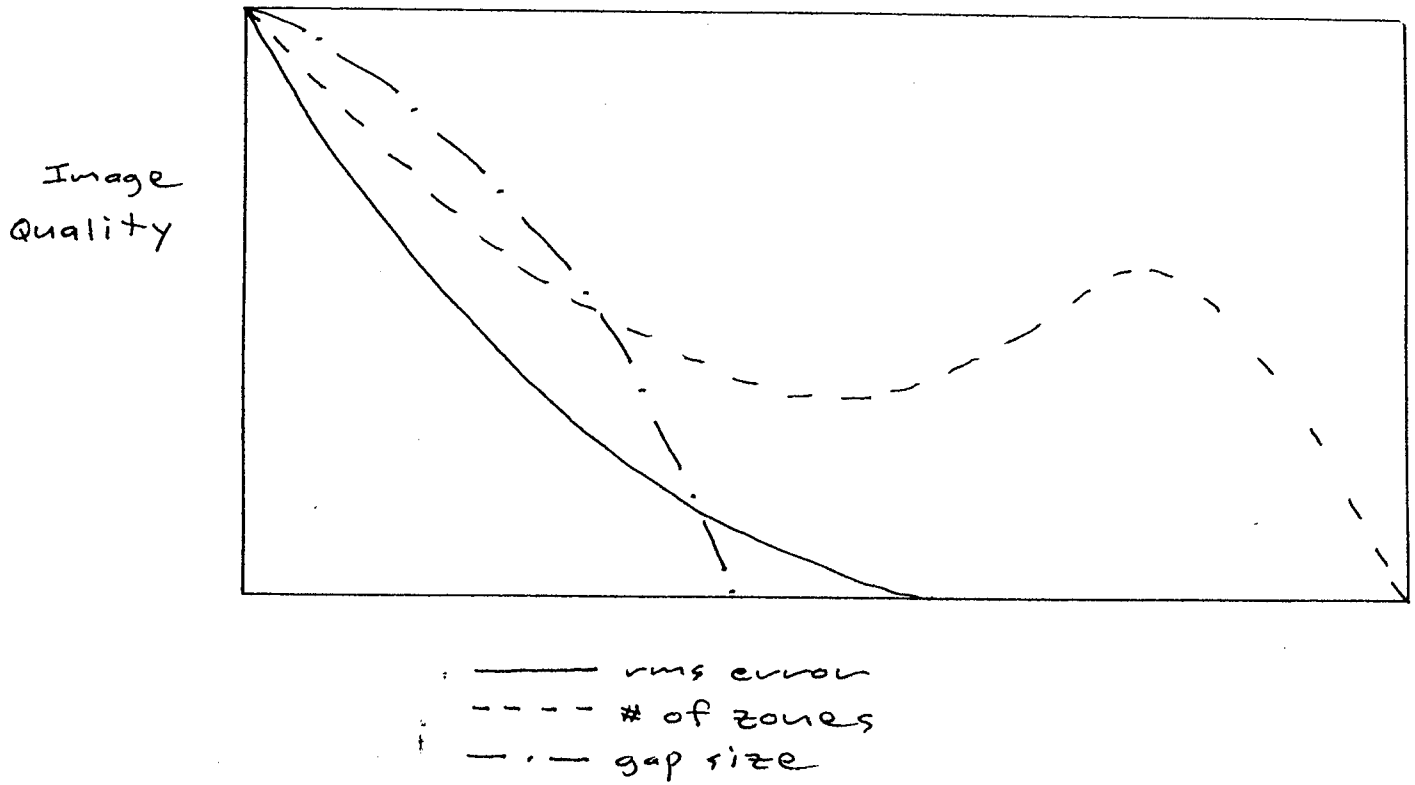

Thus, generally want large zones, fine control, and no gaps.

Summary

- Analytical model in place to perform trades on image quality versus control zone size, shape, and accuracy.
- Can be used to study segmented or continuous surfaces.
- Mathematical framework will allow future inclusion of a wider range of surface errors (such as micro roughness & figure error within a control zone).

Introduction to PSD Approach

- How can we best select a corrector for a given primary?
- Need to know magnitude of primary errors versus spatial scale (or spatial frequency) - this is the PSD of the primary.
- Then, if final image quality is specified (PSF), can select corrector that best bridges gap between primary and image.

Graphical Illustration

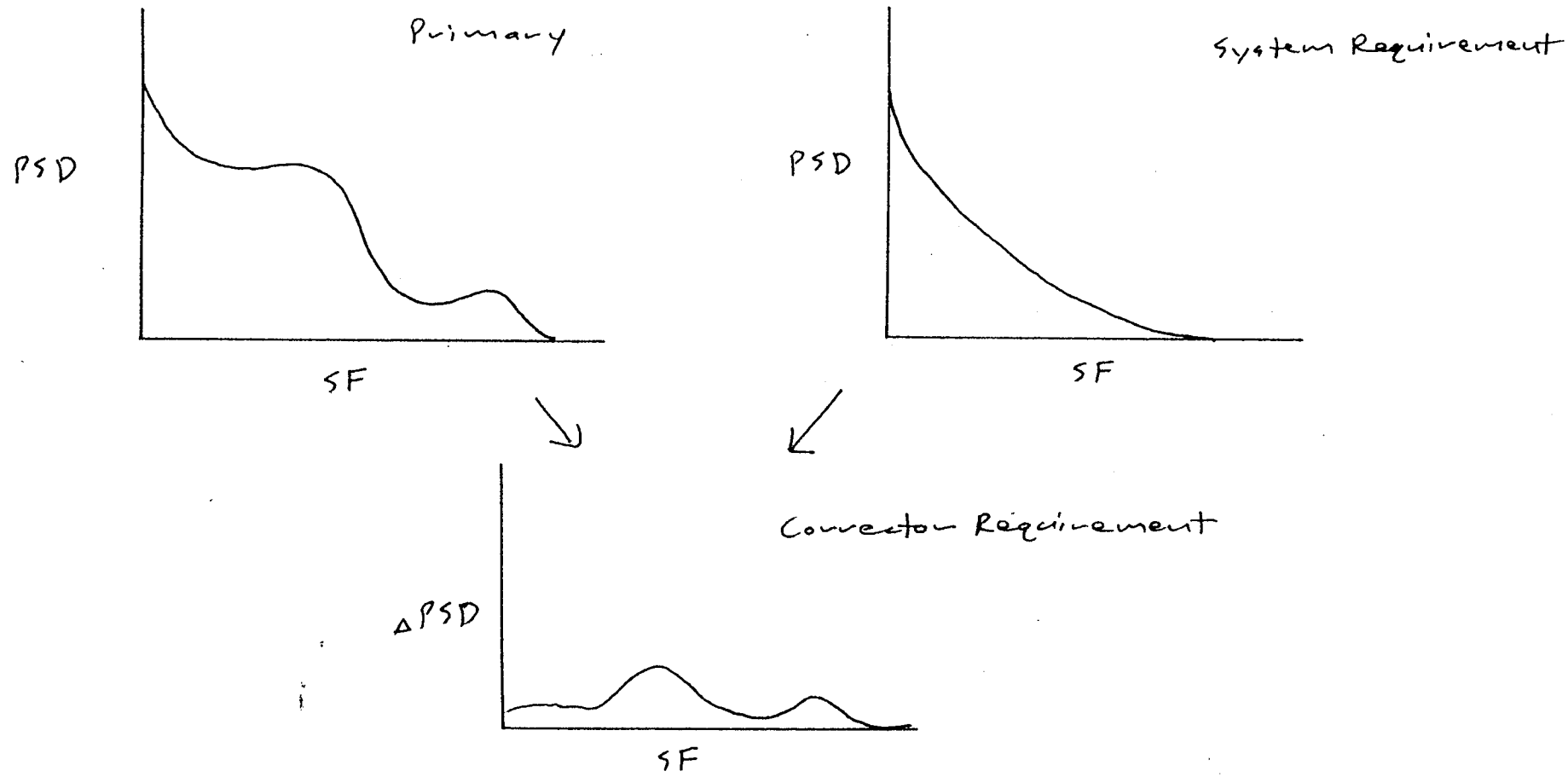

Gives required amplitude of correction (stroke) along with spatial distribution.

Tasks Required to Utilize PSD Approach

- Develop justifiable PSD's for candidate primaries (in progress).
- Develop required system PSD (from PSF) based on consensus science requirements (in progress).
- Extend to time-dependent PSD's.
- Extend to 3-dimensional PSD's.
- Develop ΔPSD's for candidate correctors (in progress).
- Match best corrector ΔPSD to required ΔPSD.

Will avoid biased, hand waving-based solutions to corrector selection problem.

NASA
National Aeronautical and Space Agency

Report Document Page

1. Report No.	2. Government Accession No.	3. Recipient's Catalog No.
1		

4. Title and Subtitle

Wavefront Analysis of Adaptive Telescope

5. Report Due

12/15/95

6. Performing Organization Code

University of Alabama in Huntsville

7. Author(s)

James B. Hadaway
Lloyd Hillman

8. Performing Organization Report No.

1

10. Work Unit No.

9. Performing Organization Name and Address

University of Alabama in Huntsville
Huntsville, Alabama 35899

11. Contract or Grant No.

NAS8-38609 D.O. 149

12. Sponsoring Agency Name and Address

National Aeronautics and Space Administration
Washington, D.C. 20546-001
Marshall Space Flight Center, AL 35812

13. Type of report and Period covered

Final

14. Sponsoring Agency Code

15. Supplementary Notes

16. Abstract

This report details work performed on the above contract.

17. Key Words (Suggested by Author(s))	18. Distribution Statement
Space telescope, optical design, active optics.	

19. Security Class. (of this report)	20. Security Class. (of this page)	21. No. of pages	22. Price
Unclassified	Unclassified	10 + appx's	

NASA FORM 1626 OCT 86

Enclosure #2